

Investigating the Relation Between Problem Hardness and QUBO Properties

Thore Gerlach¹[0000-0001-7726-1848] and Sascha Mücke²[0000-0001-8332-6169]

¹ Fraunhofer IAIS, Sankt-Augustin, Germany thore.gerlach@iais.fraunhofer.de

² Lamarr Institute, TU Dortmund University, Dortmund, Germany
sascha.muecke@tu-dortmund.de

Abstract. Combinatorial optimization problems, integral to various scientific and industrial applications, often vary significantly in their complexity and computational difficulty. Transforming such problems into Quadratic Unconstrained Binary Optimization (QUBO) has regained considerable research attention in recent decades due to the central role of QUBO in Quantum Annealing. This work aims to shed some light on the relationship between the problems' properties. In particular, we examine how the spectral gap of the QUBO formulation correlates with the original problem, since it has an impact on how efficiently it can be solved on quantum computers. We analyze two well-known problems from Machine Learning, namely Clustering and Support Vector Machine (SVM) training, regarding the spectral gaps of their respective QUBO counterparts. An empirical evaluation provides interesting insights, showing that the spectral gap of Clustering QUBO instances positively correlates with data separability, while for SVM QUBO the opposite is true.

Keywords: QUBO · Machine Learning · Spectral Gap · Quantum Computing.

1 Introduction

Combinatorial optimization problems lie at the core of many NP-hard problems in Machine Learning (ML) [7]: Clustering a data set comes down to deciding, for every point, if it belongs to one cluster or another. Training a Support Vector Machine (SVM) involves identifying the subset of support vectors (SVs). These decisions are highly interdependent, making the tasks computationally complex.

In the advent of Quantum Computing (QC), combinatorial problems have gained renewed attention due to the possibility of solving them through the exploitation of quantum tunneling effects. Particularly, the Ising model and the equivalent QUBO problem have become the central target problem class for Quantum Annealing (QA) [9,6]. In QUBO, a parameter matrix Q is given that parametrizes a loss function over binary vectors, which we want to minimize. It can be shown that, in general, this problem is NP-hard [15]. The value of QUBO lies in its versatility: Many NP-hard problems can be reduced to it by means of computing Q from input data and hyperparameters, thus QUBO has seen many

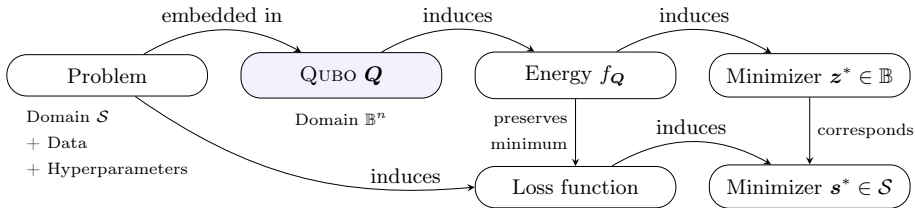


Fig. 1: Workflow of embedding a problem into QUBO. Every solution candidate s in the problem domain \mathcal{S} has an easily computable corresponding $z \in \mathbb{B}^n$.

applications in various domains [8,10,11,2,14,16,13]. Solving the QUBO formulation yields a minimizing binary vector, which maps back to an optimal solution of the original problem. Fig. 1 shows a schematic view of this workflow.

However, despite the promise of quantum speedup, not every instance of QUBO is equally easy to solve. It was shown that certain instances require exponential annealing time [1], which may render solving them on quantum computers equally infeasible as by brute force. A central determining factor is the minimal *spectral gap* (SG) of the corresponding Annealing Hamiltonian (AH), which in turn dictates the annealing speed (see Section 2): A small SG leads to a higher probability of obtaining sub-optimal results (see e.g. [17]). The SG is a physical property of the AH, and its connection to classical complexity theory is poorly understood. One would expect that classically hard problems tend to be more difficult to solve, even using non-classical methods like QA.

We investigate this connection, both by means of an empirical study and theoretical considerations. To this end, we take instances of optimization problems from ML, embed them into QUBO, and compare their properties to uncover correspondences. Our central research question is: **What is the relation between the hardness of a particular optimization problem and its corresponding QUBO formulation?** In the scope of this paper, “hardness” refers to data properties rather than complexity. We find that the relationship surprisingly not always aligns with intuition: With clustering, a stronger separation of data corresponds with a larger SG, while for SVM learning the opposite is true.

This paper is structured as follows: In Section 2, we give an overview on the background of Adiabatic QC. QUBO formulations for the two classical learning problems, Binary Clustering and SVM, can be found in Sections 3.1 and 3.2. In Section 4, we conduct experiments and a conclusion is drawn in Section 5.

2 Background

In a QUBO problem, we are given an upper triangle matrix $Q \in \mathbb{R}^{n \times n}$, which parameterizes the *energy function* f_Q defined as

$$f_Q(z) := z^\top Q z = \sum_{i=1}^n \sum_{j=i}^n Q_{ij} z_i z_j, \quad (1)$$

where $\mathbf{z} \in \mathbb{B}^n$ is a binary vector with $\mathbb{B} = \{0, 1\}$. The objective is to find a vector \mathbf{z}^* that minimizes $f_{\mathbf{Q}}$, i.e., $\forall \mathbf{z} \in \mathbb{B}^n : f_{\mathbf{Q}}(\mathbf{z}^*) \leq f_{\mathbf{Q}}(\mathbf{z})$. The Ising model is almost identical to QUBO, but uses the binary set $\mathbb{S} = \{-1, +1\}$. The model's energy function can be obtained from $f_{\mathbf{Q}}$ through a simple change of $\mathbf{z} \mapsto (\mathbf{s} + 1)/2$.

QA is a promising method for approximating the minimizing solutions of Ising models, first proposed by Kadowaki and Nishimori [9]. Instead of bits for variables it uses *qubits*, which, when measured, take either state from \mathbb{S} with a certain probability. Further, systems of n qubits can exhibit arbitrary probability distributions over the space \mathbb{S}^n .

The rough quantum-mechanical equivalent of loss functions in ML are *Hamiltonians*, which are complex-valued hermitian matrices $\mathbf{H} \in \mathbb{C}^{2^n \times 2^n}$ that describe the total energy of a system. The expected energy of an n -qubit state $|\psi\rangle$ is given by $\langle \psi | \mathbf{H} | \psi \rangle$, where $|\psi\rangle$ is a 2^n -element complex vector describing the qubits' state, and $\langle \psi |$ its conjugate transpose. The Ising model Hamiltonian is diagonal and contains the energy values for all possible binary states \mathbb{S}^n , which are simultaneously its eigenvalues. The minimizing state corresponding to the smallest eigenvalue is called *ground state*. The Adiabatic theorem states that a system with a time-dependent Hamiltonian $\mathbf{H}(t)$ tends to stay in its ground state, even if the Hamiltonian slowly changes over time [4]. At the core of QA lies the idea to prepare a quantum system in the ground state of an "easy" Hamiltonian \mathbf{H}_I and slowly change it to the actual problem Hamiltonian \mathbf{H}_P over time:

$$\mathbf{H}(s) := f(s)\mathbf{H}_I + g(s)\mathbf{H}_P, \quad (2)$$

with $f, g : [0, 1] \rightarrow \mathbb{R}_{\geq 0}$, such that $f(0) \gg g(0)$ and $f(1) \ll g(1)$. The speed at which the Hamiltonian can safely evolve without the system leaving its ground state depends on the minimal SG, which is the minimal difference between the two lowest eigenvalues over time. Let $\lambda_1(s), \dots, \lambda_{2^n}(s)$ denote the eigenvalues of $\mathbf{H}(s)$ in increasing order ($\lambda_i(s) < \lambda_{i+1}(s) \forall 1 \leq i < 2^n$), then $\gamma(\mathbf{H}(s)) := \min_{s \in [0, 1]} \lambda_2(s) - \lambda_1(s)$. When a Hamiltonian \mathbf{H} is not time-dependent, we simply write $\gamma(\mathbf{H})$ to denote the difference between its lowest eigenvalues. A small SG requires a slow change rate, which leads to a long, potentially exponential (c.f. [1]) *annealing time*. It is therefore desirable to somehow increase the SG by choosing \mathbf{H}_I , \mathbf{H}_P , f and g accordingly. As \mathbf{H}_I , f and g are usually prescribed by the annealing hardware at hand, the only free variable is \mathbf{H}_P .

When talking about the SG of a QUBO instance \mathbf{Q} , it is important to make the distinction between the parameter matrix \mathbf{Q} and its corresponding Hamiltonian $\mathbf{H}_{\mathbf{Q}}$: The entries along the diagonal of the latter correspond to the values $\mathbf{z}^\top \mathbf{Q} \mathbf{z}$ for every possible $\mathbf{z} \in \mathbb{B}^n$. Therefore, the SG is simply the difference between the lowest and second-to-lowest values of $f_{\mathbf{Q}}$ (which is very hard to compute for large n). The eigenvalues of \mathbf{Q} hold no particular relevance.

3 QUBO Formulations and their Spectral Gaps

The minimal SG $\gamma(\mathbf{H}(s))$ cannot be easily predicted from either $\gamma(\mathbf{H}_I)$ or $\gamma(\mathbf{H}_P)$. However, we can still make some statements about it using known results about eigenvalues of Hermitian matrices.

Theorem 1 (Weyl’s Inequality). *Let $\mathbf{M}, \mathbf{N}, \mathbf{R}$ be $m \times m$ Hermitian matrices with $\mathbf{N} + \mathbf{R} = \mathbf{M}$. Let μ_i, ν_i, ρ_i denote their respective eigenvalues in ascending order, i.e., $\mu_i \leq \mu_{i+1} \forall 1 \leq i < m$, and for ν_i, ρ_i analogously. Then the following inequality holds for all $1 \leq i \leq m$:*

$$\nu_i + \rho_1 \leq \mu_i \leq \nu_i + \rho_m . \quad (3)$$

Applying this inequality multiple times we find the following bound on the SG of sums of two Hamiltonians:

$$\underbrace{\mu_2 - \mu_1}_{=\gamma(\mathbf{M})} \leq \underbrace{\nu_2 - \nu_1}_{=\gamma(\mathbf{N})} + \underbrace{(\rho_m - \rho_1)}_{:=\Gamma(\mathbf{R})} . \quad (4)$$

Recall the definition of the standard time-dependent AH given in Eq. (2). Assume that $f, g : [0, 1] \rightarrow [0, 1]$, $f(0) = g(1) = 1$, $f(1) = g(0) = 0$, f is monotonous decreasing and g is monotonous increasing. E.g., f and g can be chosen as $f(s) = 1 - s$ and $g(s) = s$ with $s = t/T_a$, where T_a is the total annealing time and t the current time in the annealing process. With the assumption $f(x) = 1 - g(x)$, we obtain $\min_{s \in [0, 1]} af(s) + bg(s) = \min_{s \in [0, 1]} af(s) + b(1 - f(s)) = \min\{a, b\}$, and from Eq. (4) follows

$$\gamma(\mathbf{H}(s)) \leq \min\{\gamma(\mathbf{H}_P), \gamma(\mathbf{H}_I)\} \leq \gamma(\mathbf{H}_P) . \quad (5)$$

This result provides motivation to increase $\gamma(\mathbf{H}_P)$ when trying to improve QA performance, as it is an upper bound on $\gamma(\mathbf{H}(s))$: Increasing it does not guarantee a larger minimal SG, but is a necessary precondition.

3.1 Kernel 2-Means Clustering

Our first QUBO embedding of interest is clustering: Assume we are given a set of n data points $\mathcal{X} \subset \mathbb{R}^d$, $|\mathcal{X}| = n$. We want to partition \mathcal{X} into disjoint clusters $\mathcal{X}_1, \mathcal{X}_2 \subset \mathcal{X}$, $\mathcal{X}_1 \dot{\cup} \mathcal{X}_2 = \mathcal{X}$. We gather the data in a matrix $\mathbf{X} := [\mathbf{x}^1, \dots, \mathbf{x}^n]$, $\forall i : \mathbf{x}^i \in \mathcal{X}$, and assume that it is centered, i.e., $\mathbf{X}\mathbf{1} = \mathbf{0}$, where $\mathbf{1}$ denotes the n -dimensional vector consisting only of ones. A QUBO formulation was derived in [2], which minimizes the *within cluster scatter*:

$$\min_{\mathbf{s} \in \mathbb{S}^n} -\mathbf{s}^\top \mathbf{X}^\top \mathbf{X} \mathbf{s} \Leftrightarrow \min_{\mathbf{z} \in \mathbb{B}^n} -\mathbf{z}^\top \mathbf{X}^\top \mathbf{X} \mathbf{z} + \mathbf{1}^\top \mathbf{X}^\top \mathbf{X} \mathbf{z} , \quad (6)$$

where $\mathbf{s} = 2\mathbf{z} - \mathbf{1}$. A value $z_i = 1$ indicates that data point \mathbf{x}^i is in cluster \mathcal{X}_1 , and in \mathcal{X}_2 for $z_i = 0$. Observing that $\mathbf{X}^\top \mathbf{X}$ is a Gram matrix leads to a possible application of the kernel trick. For this, we consider a centered kernel matrix $\mathbf{K} \in \mathbb{R}^{n \times n}$ with elements $k(\mathbf{x}^i, \mathbf{x}^j)$, where $k : \mathbb{R}^n \times \mathbb{R}^n \rightarrow \mathbb{R}$ is a kernel function. $k(\mathbf{x}^i, \mathbf{x}^j)$ indicates how similar data points \mathbf{x}^i and \mathbf{x}^j are in some feature space. We can reformulate Eq. (6) to

$$\min_{\mathbf{z} \in \mathbb{B}^n} \mathbf{1}^\top \mathbf{K} \mathbf{z} - \mathbf{z}^\top \mathbf{K} \mathbf{z} \Leftrightarrow \min_{\mathbf{z} \in \mathbb{B}^n} \sum_{i, j=1}^n K_{ij} (1 - z_i) z_j \Leftrightarrow \min_{\mathcal{X}_1, \mathcal{X}_2} \sum_{\mathbf{x} \in \mathcal{X}_1, \mathbf{y} \in \mathcal{X}_2} k(\mathbf{x}, \mathbf{y}) . \quad (7)$$

We can attribute problem properties to effects on the SG of the resulting Hamiltonian of the QUBO formulation, by observing that the similarities between the different clusters are summed up. We see that the QUBO energy according to Eq. (7) is negatively correlated to the similarities within the clusters and positively correlated to the similarities between the clusters.

Thus, we claim that the SG of the QUBO formulation in Eq. (7) is (i) positively correlated to the *separability* (the inter-cluster distance), and (ii) negatively correlated to the *compactness* (the intra-cluster distances), which we validate in Section 4.1.

3.2 Simple Support Vector Machine Embedding

A linear Support Vector Machine (SVM) is a classifier that takes a labeled data set $\mathcal{D} = \{(\mathbf{x}^i, y_i)\}$ with $\mathbf{x}^i \in \mathbb{R}^d$ and $y_i \in \{-1, +1\}$ for $i \in [n] := \{1, \dots, n\}$, and separates them with a hyperplane [5]. As there may be infinitely many such hyperplanes, an additional objective is to maximize the *margin*, which is the area around the hyperplane containing no data points, in order to obtain best generalization. The hyperplane is represented as a normal vector $\mathbf{w} \in \mathbb{R}^d$ and an offset or *bias* $b \in \mathbb{R}$. To ensure correctness, the optimization is subject to $\langle \mathbf{w}, \mathbf{x}^i \rangle - b \cdot y_i \geq 1 - \xi_i$, i.e., every data point must lie on the correct side of the plane. As for real-world data perfect linear separability is unlikely, *slack variables* $\xi_i > 0$ allow for slight violations, which we want to minimize. This yields a primal objective function of

$$\begin{aligned} & \text{minimize } \frac{1}{2} \|\mathbf{w}\|_2^2 + C \sum_i \xi_i \\ & \text{s.t. } \forall i. (\langle \mathbf{w}, \mathbf{x}^i \rangle - b) \cdot y_i \geq 1 - \xi_i . \end{aligned}$$

We optimize over \mathbf{w} , b and $\boldsymbol{\xi}$, while $C > 0$ is a hyperparameter controlling the impact of misclassification. Typically this problem is solved using its well-established Lagrangian dual

$$\text{maximize } \sum_{i=1}^n \alpha_i - \frac{1}{2} \sum_{i=1}^n \sum_{j=1}^n \alpha_i \alpha_j y_i y_j \langle \mathbf{x}^i, \mathbf{x}^j \rangle \quad (8)$$

$$\text{s.t. } \sum_i \alpha_i y_i = 0, \quad 0 \leq \alpha_i \leq C \quad \forall i . \quad (9)$$

Following [14] we make the simplifying assumption that α_i can only take the values 0 or C , which allows us to introduce binary variables $z_i \in \mathbb{B}$ and write $\alpha_i = C z_i \quad \forall i$. The condition Eq. (9) can be included in the main objective by introducing the penalty term $-\lambda (\sum_i \alpha_i y_i)^2$, which is 0 when the condition is fulfilled, and negative otherwise. Similarly to the Clustering case (see Section 3.1), we can apply the kernel trick and derive the following QUBO formulation:

$$\min_{\mathbf{z} \in \{0,1\}^n} -\mathbf{1}^\top \mathbf{z} + C \mathbf{z}^\top \left(\frac{1}{2} (\mathbf{Y} \odot \mathbf{K}) + \lambda \mathbf{Y} \right) \mathbf{z} , \quad (10)$$

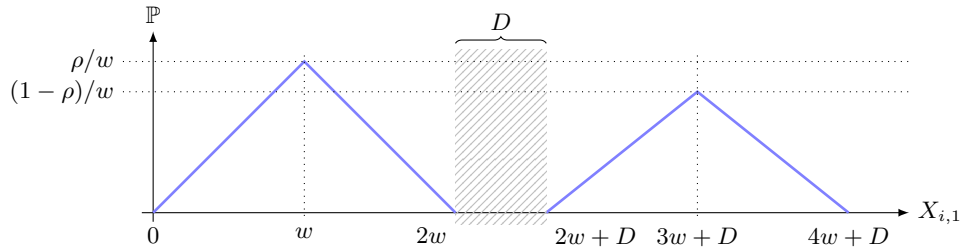


Fig. 2: Distribution of the first dimension of the 2-dimensional synthetic data used for our experiments (before applying the rotation): Two clusters are sampled such that there is a separating margin of at least size D between them. The parameter w controls the spread of data points, while r is the ratio between the number of data points in the first vs. the second cluster.

where \mathbf{Y} has entries $Y_{ij} = y_i y_j \forall i, j \in [n]$ and \odot denotes the entry-wise product. The parameter λ has to be chosen large enough to ensure Eq. (9) is fulfilled, however, if it is much larger than the objective in Eq. (8), the SG will be very small [3]. C controls how “soft” the margin is, i.e., how strongly misclassified data points are penalized. A large C does so heavily, which may result in overfitting.

We claim that the SG is negatively correlated (i) with C , (ii) with λ , and also (iii) with the *separability*, i.e., actual margin size of the data. We validate this in Section 4.2.

4 Experiments

At the core of this work we conduct an empirical evaluation of QUBO formulations and their properties. For each experiment, the steps we take are as follows: 1. Choose **problem type** and **hyperparameters**, 2. Sample **data set** with known properties, 3. Compute **QUBO parameters** and record the SG. Using the acquired data, we investigate the relationship between data parameters and SG, which has a high impact on problem hardness for QC, as we have shown before. We consider the two problems of binary clustering and SVM training, which we described in previous sections. As input data, we sample synthetic data sets for each repetition of the experiments. To this end, we consider two different types, CONES and CIRCLES, both of which have parameters allowing us to vary the resulting optimization problems’ difficulty by adjusting the data class separation.

CONES Let $n \in \mathbb{N}$ with $n \geq 2$ denote the number of data points, $\rho \in (0, 1)$ the cluster size ratio, $w > 0$ a spread parameter, and $D \in \mathbb{R}$ a separating margin size. We set $n_1 := \min\{1, \lfloor \rho n \rfloor\}$ and $n_2 := 1 - n_1$ as the cluster sizes. We create a matrix $\mathbf{X} \in \mathbb{R}^{n \times 2}$ where every entry X_{ij} is sampled i.i.d. from a triangular distribution within the interval $[0, 2w]$ and with mode w . We chose the triangular

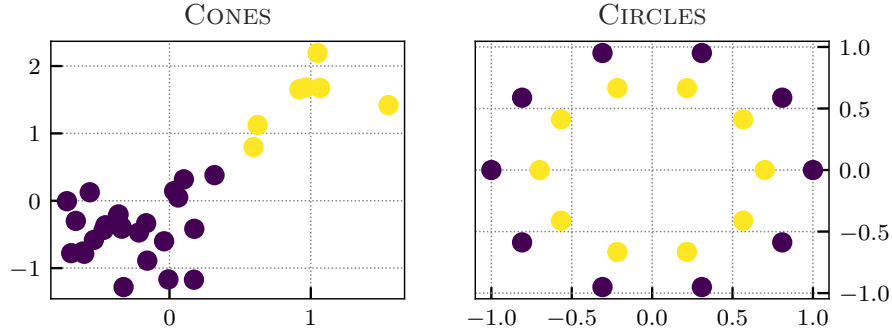


Fig. 3: Exemplary instances of the data sets used for our experiments.

distribution over a normal distribution because it has no outliers, which allows us to define a hard lower bound on the separating margin between clusters. For all $i > n_1$ we then set $X_{i,1} \mapsto X_{i,1} + 2w + D$, which shifts all of these points such that $\|\mathbf{X}_{i,\cdot} - \mathbf{X}_{\ell,\cdot}\|_2 \geq D$ is tight for all $i \in [n_1]$ and $n_1 < \ell \leq n$. The distribution of $\mathbf{X}_{\cdot,1}$ is visualized in Fig. 2; the distribution of $\mathbf{X}_{\cdot,2}$ consists of just a single triangle from 0 to $2w$ with height $1/w$ at mode w . Next, we sample θ uniformly from $[0, 2\pi)$ and apply $\mathbf{X} \mapsto \mathbf{X}\mathbf{R}(\theta)$, where $\mathbf{R}(\theta)$ is a 2D rotation matrix. This rotation leaves the distances unchanged but introduces another degree of freedom. Lastly, we center the data by computing $\boldsymbol{\mu}_j := \sum_{i=1}^n X_{ij}/n$ and applying $X_{ij} \mapsto X_{ij} - \boldsymbol{\mu}_j$ for all $i, j \in [n] \times [2]$. The target vector $\mathbf{y} \in \mathbb{S}^n$ is set to $y_i = -1$ for $i \in [n_1]$ and $y_i = +1$ for $n_1 < i \leq n$.

CIRCLES As a second data set type, we consider two circles, which are not linearly separable in \mathbb{R}^2 . The radius of the outer circle is fixed to 1 and for our experiments we vary the radius of the inner circle r . The circles consist of an equal number of points $n/2$ and Gaussian noise with standard deviation σ is added to every point (see Fig. 3, right). To bridge the gap to linear separability, we project the data set to a higher-dimensional feature space via a feature map $\phi : \mathbb{R}^2 \rightarrow \mathbb{R}^3$, $\phi(\mathbf{x}) := (x_1, x_2, a\|\mathbf{x}\|^2)^\top$. In this space, the data is linearly separable. A corresponding kernel function is given by $k(\mathbf{x}, \mathbf{y}) := \langle \phi(\mathbf{x}), \phi(\mathbf{y}) \rangle = \langle \mathbf{x}, \mathbf{y} \rangle + a^2\|\mathbf{x}\|^2\|\mathbf{y}\|^2$. For every experiment, we compare three different problem sizes, that is, we consider $n \in \{8, 20, 32\}$. To make SG comparable between QUBO instances of the same size, we scale each \mathbf{Q} such that $\|\mathbf{Q}\|_\infty = 1$.

4.1 Clustering

We first explore the Clustering QUBO in Eq. (7). Changing the maximum separating margin size between the two clusters changes the SG of the corresponding QUBO instance, as shown in Figs. 4 and 5: For Fig. 4, we sample 1000 different CONES data sets with varying cluster distances in $[0, 1]$ and fix $w = 0.2$, $\rho = 0.5$.

We find that the SG is increasing with an increasing problem size n and that

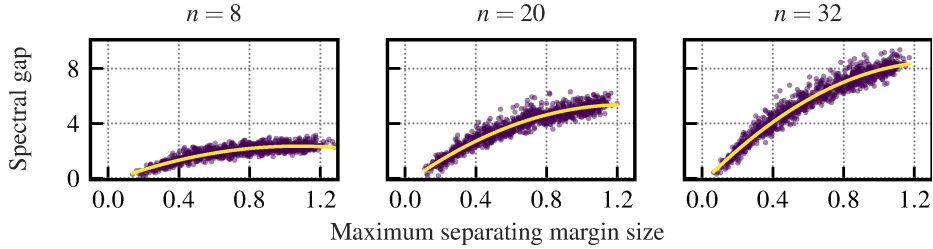


Fig. 4: Spectral gap of QUBO instances according to Eq. (7) against maximum separating margin size D for CONES; $w = 0.2$, $\rho = 0.5$ fixed, 1000 random data sets with $n \in \{8, 20, 32\}$ and $D \in [0, 1]$ uniformly sampled. The yellow curve is a fitted quadratic function.

there is a clear quadratic positive correlation between the SG and the margin size.

A similar setup can be found in Fig. 5, where 1000 different CIRCLES data sets are sampled with varying inner radius in $[0, 1]$ and $\sigma = 0.05$, $\rho = 0.5$. Again we find that the SG increases with an increasing margin size, but with a

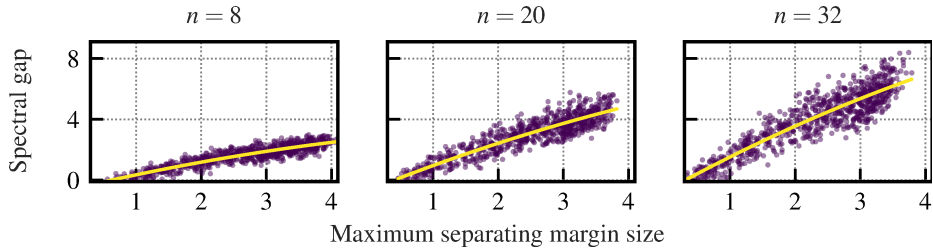


Fig. 5: Spectral gap of QUBO instances according to Eq. (7) against maximum separating margin size D for CIRCLES; $\sigma = 0.05$, $\rho = 0.5$ fixed, 1000 random data sets with $n \in \{8, 20, 32\}$ and $r \in [0, 1]$ uniformly sampled. The yellow curve is a fitted quadratic function.

linear correlation. Since different kernels are used in Fig. 4 and Fig. 5, the exact correlation form is dependent on the exact data set and the used kernel.

In Fig. 6, the effects of a varying cluster ratio in $\rho \in [0.1, 0.5]$ are depicted for the CONES setup. We again sample 1000 data sets with fixing $w = 0.2$ and $D = 0.5$. A positive correlation becomes evident between cluster ratio and SG. That is, the QUBO problem is easier to solve with QC when the clusters have the same size. The effect that the plots look like a step function for small n is

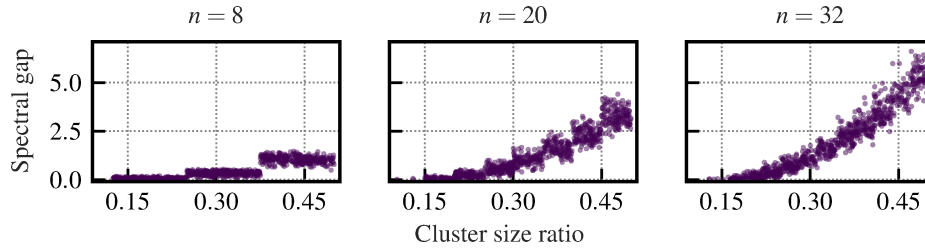


Fig. 6: Spectral gap of QUBO instances according to Eq. (7) against cluster ratio for CONES; $D = 0.5$, $w = 0.2$ fixed, 1000 random data sets for $n \in \{8, 20, 32\}$ and $\rho \in [0.1, 0.5]$ uniformly sampled.

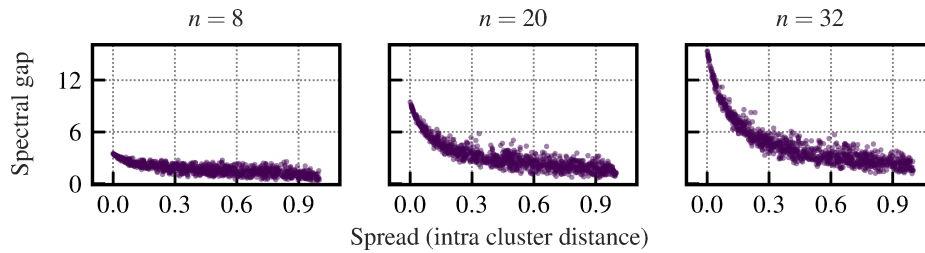


Fig. 7: Spectral gap of QUBO instances according to Eq. (7) against spread for CONES; $D = 0.5$, $\rho = 0.5$ fixed, 1000 random data sets for $n \in \{8, 20, 32\}$ and $w \in [0, 1]$ uniformly sampled.

due to the fact that there $n/2$ different configurations, e.g., for $n = 8$, we can have the four cases $n_1 = 1$, $n_1 = 2$, $n_1 = 3$ and $n_1 = 4$.

In Fig. 7, we vary the spread $w \in [0, 1]$ for 1000 different data sets and fix $D = 0.5$, $\rho = 0.5$. We can see that the SG is negatively correlated to the spread of the data set.

Putting the results together we can deduce that the is SG positively correlated with the inter-cluster distance (separability) and negatively correlated with the intra-cluster distance, supporting our claims in Section 3.1.

4.2 Support Vector Machine

We move over to experiments with the SVM QUBO in Section 3.2. Again, we depict the effect of changing the maximum separating margin size between the two clusters on the SG of the corresponding QUBO in Figs. 8 and 9. We use the same parameters for the data sets as in Figs. 4 and 5. Interestingly, we now observe a negative correlation between the SG and the margin size, making the problem harder to solve with a quantum computer if the data is well separable. For $n = 32$ the spectral basically vanishes from a certain margin size for CIRCLES. Furthermore, we again observe that this correlation is quadratic for CONES and

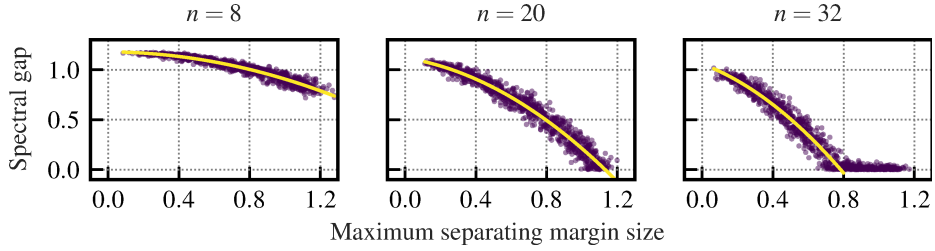


Fig. 8: Spectral gap of QUBO instances according to Eq. (10) against maximum separating margin size D for CONES. Same configuration as for Fig. 4.

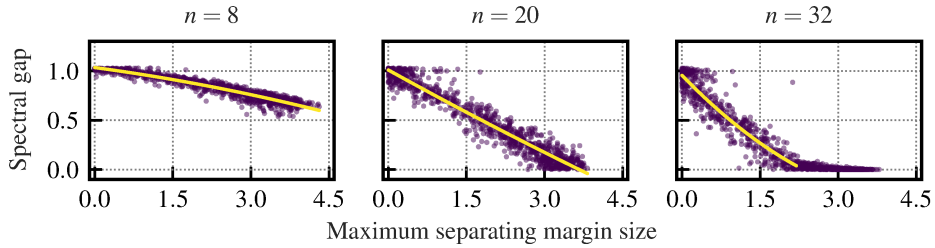


Fig. 9: Spectral gap of QUBO instances according to Eq. (10) against maximum separating margin size D for CIRCLES. Same configuration as for Fig. 5.

linear for CIRCLES, leading to a large dependence on the used kernel function and the data set at hand.

Note that we are considering a QUBO formulation for a soft-margin SVM: even though the SG might be very small, the second best solution might also be satisfactory for solving the original problem. In contrast, the second best solution of a Clustering QUBO is much worse: changing a single bit leads to a data point within the wrong cluster, which increases the energy more dramatically the further the two clusters are separated.

In Figs. 10 and 11, we show the effect of varying λ and C on the SG for CONES. We fix $\rho = 0.5$, $w = 0.2$, $D = 0.5$ and sample 10 000 data sets with $C \in [0, 0.1]$, $\lambda \in [0, 100]$ for Fig. 10 and $\lambda \in [0, 10]$ for Fig. 11, respectively. It is evident from Fig. 10 that the SG decreases as λ and C are increased. However, there are interesting intervals for λ when fixing C , such that the SG first increases and then decreases with increasing λ , forming a triangular shape when plotted, which gets more pointy with an increasing value of C – see Fig. 11 for a closer view. We observe a similar effect with CIRCLES.

Combining our observations we deduce that the SG is negatively correlated with the inter-cluster distance (separability) and the parameters λ , C except for a small region, supporting our claims from Section 3.2.

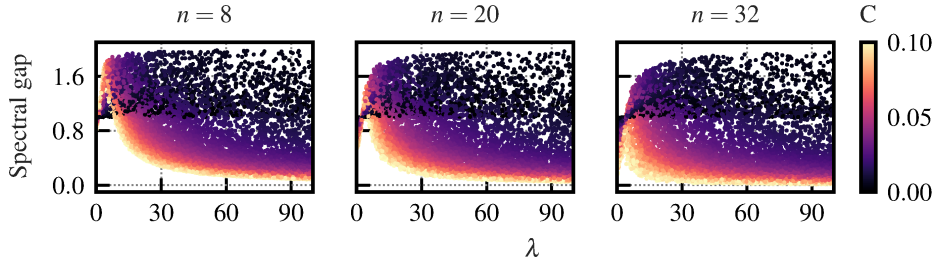


Fig. 10: Spectral gap of QUBO instances according to Eq. (10) against λ and C for CONES; $w = 0.2$, $\rho = 0.5$ fixed, 10 000 random data sets for $n \in \{8, 20, 32\}$ and $\lambda \in [0, 100]$, $C \in [0, 0.1]$ uniformly sampled.

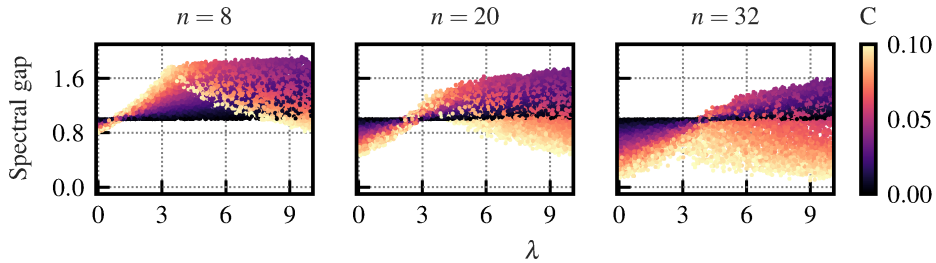


Fig. 11: Same as Fig. 10, zoomed in on $\lambda \in [0, 10]$.

5 Conclusion

In this paper, we investigated the connection between the problem hardness of classical ML problems and their solvability on quantum hardware. We considered QUBO formulations for the 2-Means Clustering and SVM learning. We highlighted that the SG of these formulations impact their solvability on quantum hardware, and showed how the SG behaves when adapting the problem parameters, which we underpinned with an empirical study.

We found that for 2-Means Clustering an easier problem also leads to a better solvability on quantum computers. Here, “easy” refers to the separability and compactness of the different classes. We found a positive correlation between these properties and the SG of the corresponding QUBO. Interestingly, this is not the case for the SVM problem, where we would expect a better solvability of a problem with a large separation of the classes. However, we found a negative correlation between separation and SG. Furthermore, other hyperparameters, such as the one controlling the softness of the margin avoiding overfitting, are negatively correlated to the SG. This is due to the balancing different objectives in one single QUBO problem. Combining these two insights, we conclude that the original problems’ hardness is not directly connected to the solvability on quantum computers, as one might assume. Instead, it depends not only on the data set at hand, but also on specifics in the used QUBO formulation. It would be in-

sightful to compare the properties of more QUBO formulations of more problems in future work. Furthermore, investigating the effect of the QUBO parameters and not only the problem parameters is an interesting research direction [12]. This could strengthen our intuition about which problems are hard for quantum computers in particular, and the potential and limitations of QC in general.

References

1. Altshuler, B., Krovi, H., Roland, J.: Adiabatic quantum optimization fails for random instances of NP-complete problems. arXiv:0908.2782 [quant-ph] (Dec 2009)
2. Bauckhage, C., Ojeda, C., Sifa, R., Wrobel, S.: Adiabatic quantum computing for kernel $k=2$ means clustering. In: LWDA. pp. 21–32 (2018)
3. Benkner, M.S., Golyanik, V., Theobalt, C., Moeller, M.: Adiabatic quantum graph matching with permutation matrix constraints. In: 2020 International Conference on 3D Vision (3DV). pp. 583–592. IEEE (2020)
4. Born, M., Fock, V.: Beweis des Adiabatsatzes. *Zeitschrift für Physik* **51**(3), 165–180 (Mar 1928). <https://doi.org/10.1007/BF01343193>
5. Cortes, C., Vapnik, V.: Support-vector networks. *Machine Learning* **20**(3), 273–297 (Sep 1995). <https://doi.org/10.1007/BF00994018>
6. Farhi, E., Goldstone, J., Gutmann, S., Sipser, M.: Quantum computation by adiabatic evolution. arXiv preprint quant-ph/0001106 (2000)
7. Guruswami, V., Raghavendra, P.: Hardness of learning halfspaces with noise. *SIAM Journal on Computing* **39**(2), 742–765 (2009)
8. Hammer, P.L., Shlifer, E.: Applications of pseudo-Boolean methods to economic problems. *Theory and decision* **1**(3), 296–308 (1971)
9. Kadowaki, T., Nishimori, H.: Quantum annealing in the transverse Ising model. *Physical Review E* **58**(5), 5355 (1998)
10. Kochenberger, G., Glover, F., Alidaee, B., Lewis, K.: Using the unconstrained quadratic program to model and solve Max 2-SAT problems. *International Journal of Operational Research* **1**(1-2), 89–100 (2005)
11. Kochenberger, G., Hao, J.K., Glover, F., Lewis, M., Lü, Z., Wang, H., Wang, Y.: The unconstrained binary quadratic programming problem: A survey. *Journal of Combinatorial Optimization* **28**(1), 58–81 (2014)
12. Mücke, S., Gerlach, T., Piatkowski, N.: Optimum-preserving qubo parameter compression. arXiv preprint arXiv:2307.02195 (2023)
13. Mücke, S., Heese, R., Müller, S., Wolter, M., Piatkowski, N.: Feature selection on quantum computers. *Quantum Machine Intelligence* **5**(1) (2023). <https://doi.org/10.1007/s42484-023-00099-z>
14. Mücke, S., Piatkowski, N., Morik, K.: Learning Bit by Bit: Extracting the Essence of Machine Learning. In: Proceedings of the Conference on "Lernen, Wissen, Daten, Analysen" (LWDA). CEUR Workshop Proceedings, vol. 2454, pp. 144–155 (2019)
15. Pardalos, P.M., Jha, S.: Complexity of uniqueness and local search in quadratic 0–1 programming. *Operations research letters* **11**(2), 119–123 (1992)
16. Piatkowski, N., Gerlach, T., Hugues, R., Sifa, R., Bauckhage, C., Barbaresco, F.: Towards bundle adjustment for satellite imaging via quantum machine learning. In: 2022 25th International Conference on Information Fusion (FUSION). pp. 1–8. IEEE (2022)
17. Somma, R.D., Boixo, S., Barnum, H., Knill, E.: Quantum Simulations of Classical Annealing Processes. *Physical Review Letters* **101**(13), 130504 (Sep 2008). <https://doi.org/10.1103/PhysRevLett.101.130504>